Journal of Power Sources 188 (2009) 184–191

Contents lists available at ScienceDirect

Journal of Power Sources

journal homepage: www.elsevier.com/locate/jpowsour

Validity of two-phase polymer electrolyte membrane fuel cell models with respect to the gas diffusion layer

C. Ziegler[a,*], D. Gerteisen[b]

[a] Laboratory for MEMS Applications, Department of Microsystems Engineering – IMTEK, University of Freiburg, Georges-Koehler-Allee 106, D-79110 Freiburg, Germany
[b] Fraunhofer Institute for Solar Energy Systems, Heidenhofstr. 2, D-79110 Freiburg, Germany

ARTICLE INFO

Article history:
Received 18 August 2008
Received in revised form 30 October 2008
Accepted 16 November 2008
Available online 27 November 2008

Keywords:
Proton exchange membrane fuel cell
Two-phase model
Validity
GDL

ABSTRACT

A dynamic two-phase model of a proton exchange membrane fuel cell with respect to the gas diffusion layer (GDL) is presented and compared with chronoamperometric experiments. Very good agreement between experiment and simulation is achieved for potential step voltammetry (PSV) and sine wave testing (SWT). Homogenized two-phase models can be categorized in unsaturated flow theory (UFT) and multiphase mixture (M^2) models. Both model approaches use the continuum hypothesis as fundamental assumption. Cyclic voltammetry experiments show that there is a deterministic and a stochastic liquid transport mode depending on the fraction of hydrophilic pores of the GDL. ESEM imaging is used to investigate the morphology of the liquid water accumulation in the pores of two different media (unteflonated Toray-TGP-H-090 and hydrophobic Freudenberg H2315 I3). The morphology of the liquid water accumulation are related with the cell behavior. The results show that UFT and M^2 two-phase models are a valid approach for diffusion media with large fraction of hydrophilic pores such as unteflonated Toray-TGP-H paper. However, the use of the homgenized UFT and M^2 models appears to be invalid for GDLs with large fraction of hydrophobic pores that corresponds to a high average contact angle of the GDL.

1. Introduction

Fuel cells are considered to be promising energy converters due to their high conversion efficiency, minimal noise and environmental friendliness. Of the various types of fuel cells, the polymer electrolyte membrane fuel cell (PEMFC) is the most versatile type for mobile, transportation and CHP applications. The necessity to use limited energy resources efficiently is made more urgent by climate change and a growing global population. For the PEMFC, an understanding of the formation and transport of liquid water that is associated with the evolution of two-phase flow is a key to increased cell performance and enhanced durability.

A major contribution to this fundamental understanding is provided by two-phase models that have been attempted by many different authors. Wang and co-workers described the two-phase flow using a two-phase mixture approach where the governing equations contain fluid properties that depend on the mixture composition and the degree of saturation [1]. The model includes the assumption that the GDL can be described by effective averaged material properties. Berning and Djilali published a three- dimensional two-phase model considering the anode and cathode sides [2]. A study on the impact of operating conditions on the saturation is presented in [3]. Ref. [4] presents a non-isothermal two-phase model focusing on the interaction between heat and two-phase transport. Birgersson and Vynnycky presented a scale analysis of a complete two-phase model [5]. They also showed the large impact of different assumptions regarding saturation-dependent parameters on the predicted saturation level. An approach to determine the saturation-dependent transport parameters of GDLs by using the pore-morphology method in combination with lattice Boltzmann methods is presented in Ref. [6]. Nam et al. investigated the influence of saturation on the effective diffusivity and cell performance including the aspects of material properties and phase transition rates [7]. A theoretical study of a two-layer diffusion medium is given. They assume a branching-type geometry for the microscopic to macroscopic water transport. In Ref. [8], a similar approach is adopted and the importance of treating the catalyst layer as a separate domain is highlighted on the basis of modeling results. Markicevic and Djilali provided a theoretical investigation of the two-scale transport in porous media including the three different regimes of Darcy, Brinkmann and Stokes flow [9]. A fractal approach for the transport properties of GDLs including a comparison with experimental data is presented in Ref. [10]. The authors study the influence of various fractions of hydrophilic pores in otherwise hydrophobic media. In Ref. [11], special emphasis is placed

* Corresponding author. Tel.: +49 761 203 7447; fax: +49 761 203 7539.
E-mail address: christoph.ziegler@imtek.de (C. Ziegler).
URL: http://www.imtek.de (C. Ziegler).

0378-7753/$ – see front matter © 2008 Elsevier B.V. All rights reserved.
doi:10.1016/j.jpowsour.2008.11.071

Nomenclature

a	active area of cathode ($1\,m^{-1}$)
d	Nam-Kaviany parameter
d_c	thickness of cathode ($10\,\mu m$)
d_{gdl}	thickness of GDL ($280\,\mu m$)
D_{O_2}	diffusivity of oxygen ($m^2\,s^{-1}$)
$D^0_{O_2}$	vacuum diffusivity of oxygen ($1.8 \times 10^{-5}\,m^2\,s^{-1}$)
F	Faraday constant ($96485\,C\,mol^{-1}$)
j_0	exchange current density ($A\,m^{-2}$)
k_{rel}	relative permeability
m	van Genuchten parameter
M_l	molar mass of water ($0.018\,kg\,mol^{-1}$)
M_{O_2}	molar mass of oxygen ($0.032\,kg\,mol^{-1}$)
p_l	liquid water pressure (Pa)
p_g	gas pressure (Pa)
p_d	entry pressure (Pa)
R	universal ga constant ($8.314\,J\,(kg\,mol)^{-1}$)
s_l	liquid water saturation
T	temperature
x_{O_2}	molar fraction of oxygen
z	number of electrons involved in ORR

Greek symbols

α	symmetry factor
β	coupling parameter
γ	van Genuchten parameter
δ	Nam-Kaviany parameter
η_c	cathode overpotential (V)
π	porosity of the GDL
ρ_l	mass density of liquid water ($kg\,m^{-3}$)

on the conditions at the boundary between the GDL and the open gas channel. The liquid water motion in the gas channels is investigated using CFD in Ref. [12]. The dry–wet transition in the GDL is investigated in [13]. The results show that the multi-phase mixture approach can capture the dry–wet–dry transition in a fixed grid. Yu et al. presented a model-based evaluation of NR data [14]. Good correlation between simulation and NR data is found indicating that the two-phase approach might be valid. In Ref. [15] a one-dimensional non-isothermal transient model is described by Shah et al. It explains the hysteresis frequently observed in experiments therefore providing a tool for MEA screening. The work of Shah and co-workers represents an extension of an approach previously developed in [16,17]. This approach is based on the combination of voltammetry measurements and dynamic modeling.

In the literature there are large differences regarding the simulated liquid saturation of the GDL, depending on the functional form of the saturation-dependent parametrizations and the material parameters that are used. Different authors predict a maximum liquid saturation of 1 [18], 0.25 [19] and 0.09 [2] a situation that highlights the qualitative character of current two-phase studies. In this paper, the validity of current two-phase models is discussed with a focus on the description of the porous GDL. A brief discussion and overview of the common saturation-dependent parameterizations for capillary pressure, permeability and diffusivity are given. For the purpose of model validation and two-phase parameter extraction by inverse modeling, we fit a dynamic two-phase model of the GDL to chronoamperometric measurements of the type presented in [20]. The two-phase behavior of different GDL materials (untreated Toray TGP-H-090 and Freudenberg H2315 I3) is compared. This is done using potential sweep experiments and environmental scanning electron microscope (ESEM) imaging, which allows the observation of liquid water inside the pores of the GDL. The results of the model validation study are interpreted in the light of the potential sweeps and microscopic two-phase images. The validity and limitation of two-phase and multi-phase mixture PEMFC models based on the continuum hypothesis are discussed.

2. Dynamic two-phase GDL model

A model of the capillary-driven water transport in the cathodic GDL is presented and compared with two different chronoamperometric experiments namely a potential-step measurement and a sine-wave test. The model is time-dependent, one-dimensional and isothermal. The GDL is spatially resolved along the through-plane direction. The catalyst layer and the gas channel are described in terms of boundary conditions. A detailed description of the oxygen diffusion and the capillary transport of liquid water through the GDL is provided. The oxygen reduction reaction is described using the Tafel equation. An important part of the model is the coupling of the liquid water transport with the oxygen diffusion and the electrochemical reaction. The parameters involved in these couplings and in the capillary transport are important for the quantitative comparison of the simulation results with experimental data. The speed of convergence of an implicit solution procedure depends on the number of degrees of freedom, which is low in the case of a one-dimensional model. To date, most of the two-dimensional and three-dimensional two-phase models failed to demonstrate the capability of dynamic simulations on technically relevant time scales due to limitations inherent in the numerical solution procedures. The current limit of simulated operation time is given by a recent publication where 22.75 s of a drying process is simulated for a GDL exposed to dry gas [21]. However, the computational effort for such a model is not compatible with numerical optimization that requires iteratively repeated calculations with the fuel cell model.

The most fundamental assumption of the model presented here is the description of the transport through the GDL based on the continuum hypothesis. The field representation is used for the state variables. The GDL is described by spatially averaged effective transport properties. The continuum assumption however considers fluids and the GDL to be continuous. That is, properties such as density, pressure, temperature, velocity and material properties of the GDL are taken to be well-defined at "infinitely" small points, defining a REV (Reference Element of Volume), at the geometric order of the distance between adjacent nodes in the computational grid. Properties are assumed to vary continuously from one point to another, and are averaged values in the REV. While the fact that the fluid is made up of discrete molecules can be ignored ($Kn \ll 1$) the continuum hypothesis is basically an approximation and therefore results in approximate solutions. Consequently, assumption of the continuum hypothesis can lead to results which are not of the desired accuracy. The continuum hypothesis is used in many previous publications on two-phase and multi-phase mixture modeling of fuel cells, e.g. [1–5,13,15].

Additional model assumptions are made here: the model is isothermal. The measurement results were taken from an isothermal test cell that was cooled by a very high flux of coolant. In [20] it was shown that the inevitable small variation of temperature under operation does not obscure the footprint of the liquid water transport. The gas pressure in the GDL is assumed to be constant. The Peclet number for the gas transport in the GDL is estimated in Ref. [5]. Unless there are larger pressure gradients between adjacent channels, the gas convection can be neglected. Lateral transport along the in-plane direction – in particular the difference between channel and intermediate areas – is neglected. The model describes

the two-phase regime where liquid water exists in the GDL and the gas phase is assumed to be saturated. Water enters the GDL in the liquid phase and the phase change is not taken into account. The liquid water transport is governed by the balance of the liquid saturation s_l, that is

$$\pi\rho_l \frac{\partial s_l}{\partial t} + \nabla\cdot(\rho_l v_l) = 0 \tag{1}$$

where π denotes the porosity of the GDL and ρ_l the liquid density. v_l describes the liquid velocity component in the through-plane direction. The velocity is given by Darcy's law

$$v_l = -\frac{1}{\mu_l} k_{r,l} K_{int} \nabla p_l \tag{2}$$

where the liquid pressure is given by $p_l = p_g - p_c$. For the relative permeability and the capillary pressure the parametrizations according to van Genuchten are used:

$$k_{r,l}(s_l) = s_l^{\gamma}[1-(1-s_l)^{1/m}]^{2m}, \tag{3}$$

$$p_c(s_l) = p_d[(1-s_l)^{-1/m}-1]^{1-m}. \tag{4}$$

The oxygen diffusion is described by

$$\pi\rho_{O_2}\frac{\partial x_{O_2}}{\partial t} - \nabla\cdot(\rho_{O_2} D_{O_2}\nabla x_{O_2}) = 0 \tag{5}$$

where ρ_{O_2} denotes the density and x_{O_2} is the molar fraction of oxygen. The diffusivity D_{O_2} is described using

$$D_{O_2} = D^0_{O_2}(1-s_l)^{\delta}\pi\left(\frac{\pi-0.11}{1-0.11}\right)^d. \tag{6}$$

The oxygen reduction reaction at the cathode side is modeled by the Tafel equation. To account for the porous structure of the catalyst layer, the active surface area per unit volume a is introduced. The current density is described by

$$j_c = -(1-s_l)^{\beta} d_c a j_0 x_{O_2} \exp\left(\frac{-\alpha z F \eta_c}{RT}\right) \tag{7}$$

where d_c denotes the thickness of the catalyst layer. The term $(1-s_l)^{\beta}$ couples the current density and the liquid saturation at the interface between the GDL and the catalyst layer to account for the fact that increased saturation reduces the active surface area of the catalyst layer. At the interface between the GDL and the gas channel, the following Dirichlet boundary conditions apply:

$$s_l = 0, \tag{8}$$

$$x_{O_2} = 0.21. \tag{9}$$

Neumann boundary conditions apply at the interface between the GDL and the catalyst layer:

$$N_l = \frac{M_l}{2F}\cdot j_c, \tag{10}$$

$$N_{O_2} = -\frac{M_{O_2}}{4F}\cdot j_c. \tag{11}$$

The solution method, the optimization scheme and the determination of the initial paramete set by numerical upscaling are described in detail in Ref. [22]. The experimental details of the chronoamperometric measurements that are used for comparison with simulation results are described in Ref. [20].

3. Comparison with experimental results

In Fig. 1 simulation and measurement are compared for a potential step experiment. A voltage step from 0.59 V to 0.06 V was applied at $t = 0$. The resulting current response of the cell is shown in Fig. 1. The fitted simulation result shows very good agreement

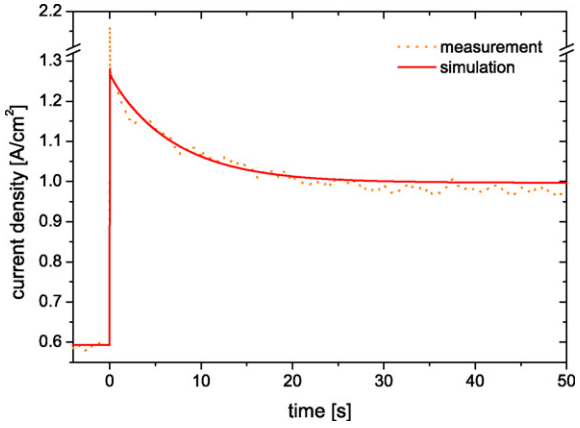

Fig. 1. The measured current density and the simulated current density are compared for a potential step voltammetry (PSV) experiment.

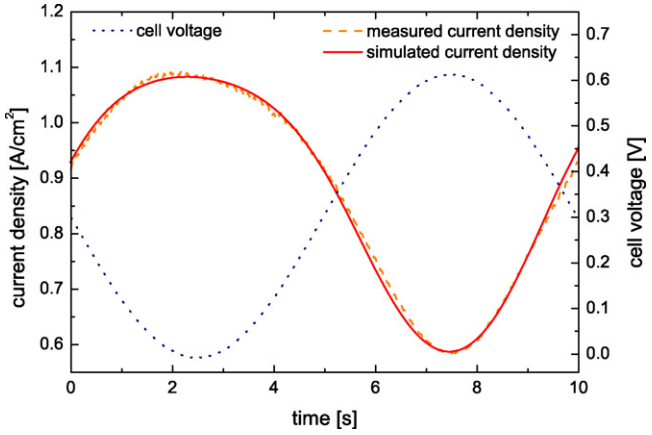

Fig. 2. Comparison of measured current density and fitted simulated current density for the sine wave testing (SWT) experiment.

with the experimental data. Alternatively, the liquid water transport within a GDL can be excited using sine-wave perturbations at low frequencies in combination with large amplitudes. The result of such an experiment is shown in Fig. 2. Again excellent agreement between experiment and simulation is achieved. The corresponding saturation change and oxygen concentration are shown in Figs. 3 and 4 for the potential-step experiment and the sine-wave testing. Note that the liquid saturation predicted by the model is

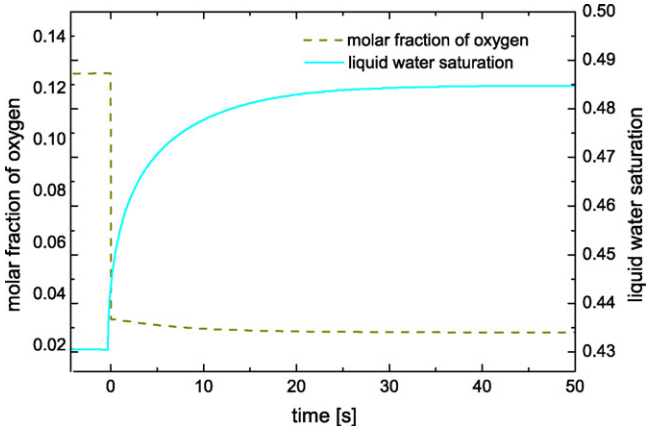

Fig. 3. Time evolution of liquid water saturation and molar fraction of oxygen at the boundary between GDL and cathode catalyst layer. The increase in the liquid saturation of the GDL causes the decrease in current density in Fig. 1.

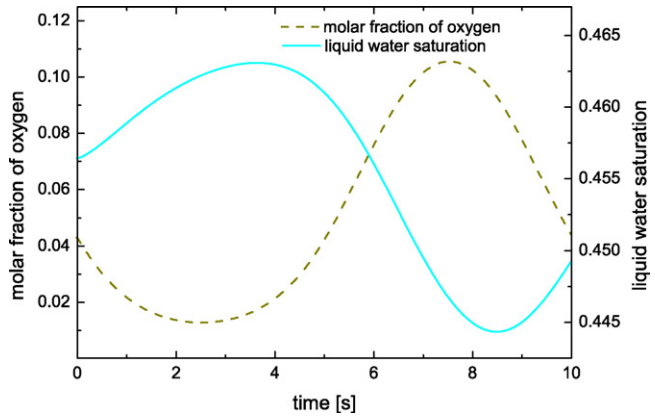

Fig. 4. Evolution of liquid water saturation and molar fraction of oxygen for the SWT experiment (Fig. 2).

Table 1
Kinetic parameters.

Symbol	PSV	SWT
aj_0 (A m^{-3})	1.6×10^9	1.9×10^9
α	0.14	0.14
T (K)	313	315

Table 2
Two-phase parameters.

β	0.62	0.50
γ	1.82	1.86
d	0.55	0.61
δ	3.34	3.42
m	0.76	0.75

in the range between 0.4 and 0.5, so is significantly higher than modeling results based on the use of standard literature values for the two-phase description (see e.g. Ref. [22], Fig. 5 therein). In Ref. [20] we estimated and discussed the saturation change due to increased product water generation resulting from a similar potential step experiment to be between 0.01 and 0.03. For comparison we extract a saturation change of 0.05–0.06 from the simulation results in Fig. 3. The relative change of the saturation is in good agreement with the experimental evidence. Simulation results and experiment show that a small change in the saturation changes the fuel cell performance significantly. This highlights the importance and potential of the micro water management in the GDL. Untreated Toray TGP-H-090 paper was used in both experiments.

In Table 1, the extracted material parameters are listed for the potential step voltammetry (PSV) and the since wave testing (SWT) experiments. The two-phase and coupling parameters appearing in the van Genuchten formulas (Eqs. (4) and (3)), the description of the diffusivity (Eq. (6)) and the current density (Eq. (7)) are listed in Table 2. Good agreement is found between the two different experiments (Table 3). A detailed discussion and analysis of the model parameters is given in Ref. [22].

Table 3
Material parameters.

K_{int}	1.2×10^{-11}	1.2×10^{-11}
p_d	−0.99	−1.10
π	0.51	0.50

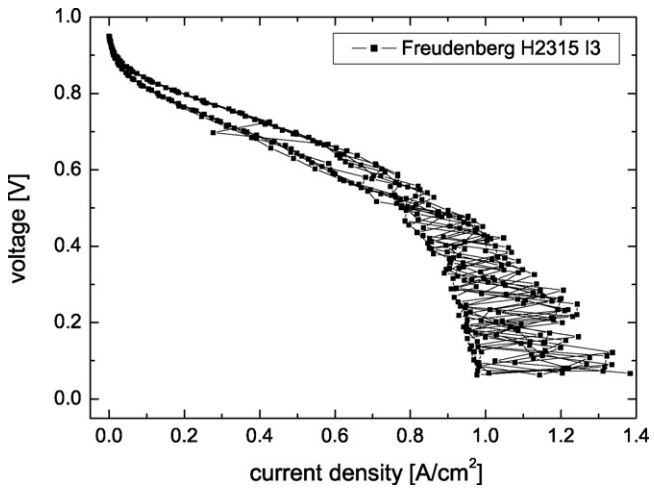

Fig. 5. Cyclic voltammogram with scan rate of 10 mV s^{-1}. The hydrophobic Freudenberg H2315 I3 GDL is used. The current density shows stochastic behavior in the two-phase regime. This corresponds to a liquid water distribution in form of droplets and individual transport channels (Fig. 7c).

4. Validity and limitations of existing two-phase models

However there are significant differences in the behavior of the fuel cell in chronoamperometric experiments, depending on the type of GDL material in use. To investigate this, we compared the fundamental behavior of two different materials (Toray TGP-H-090 and Freudenberg H2315 I3). Commonly, the carbon-fiber based diffusion media rely on a co-polymer containing mainly polyacrylanitrile. The Toray paper belongs to the group of non-woven wet-laid carbon-fiber papers. After heat treatment, it consists of carbon fibers held together by a carbon matrix. The TGP-H-090 end product is characterized by straight fibers and comparatively large pores. We used a water column test to measure the bubble point, i.e. the point at which a continuous liquid path through the GDL exists, and determined a value of 4.7 kPa. The uncompressed porosity of the material is 0.78 where the hydrophilic porosity was determined to be 0.63 [23]. The surface contact angle is 134° measured with the sessile drop method. Another production approach is represented by dry-laid polyacrylanitrile fibers that form a thin fleece which is bound by hydroentangling. This creates a mechan-

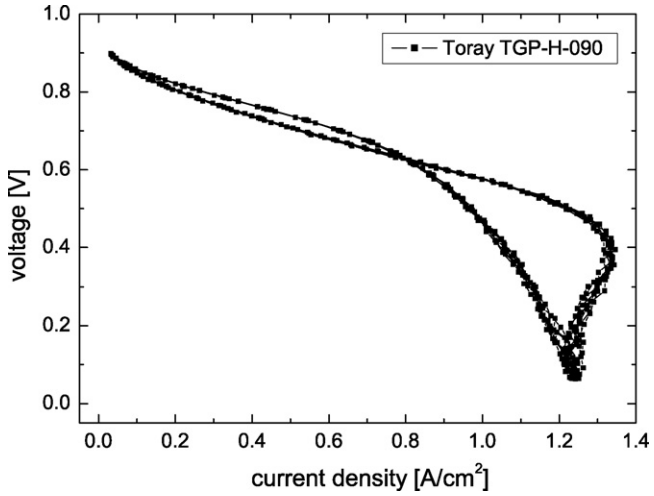

Fig. 6. Cyclic voltammogram with untreated Toray TGP-H-090 (scan rate 10 mV s^{-1}). The current density shows time-continuous behavior in the two-phase regime. The liquid water distribution in the GDL is weakly influenced by the pore morphology of the GDL (Fig. 8c).

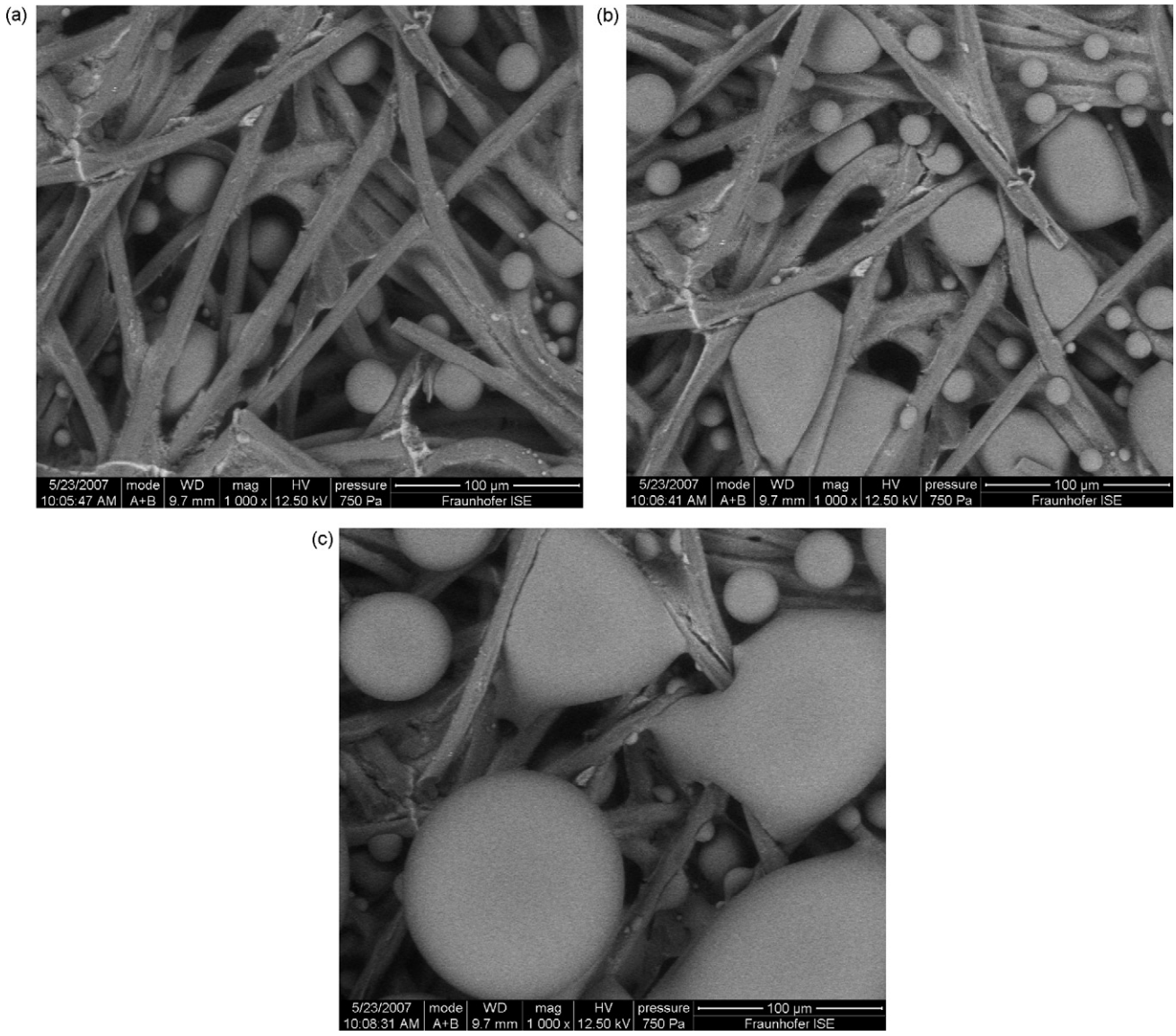

Fig. 7. ESEM images of liquid water in a hydrophobic Freudenberg H2315 I3 GDL. Water droplets form and start filling the cavities (a). Subsequently, the droplets merge partially to form larger droplets (b). Eventually, a few large droplets and liquid films with high curvature and surface shapes governed by the pore morphology appear (c).

ically bonded non-woven fabric. The Freudenberg H2315 I3 GDL belongs to this group of material. We measured the bubble point to be 4.9 kPa, slightly higher than for the Toray paper and thus indicating a smaller maximum pore diameter or higher internal contact angle. The surface contact angle was determined to be 133° using the sessile drop method. As known from earlier work [16], the fundamental behavior of a GDL in the two-phase regime can be detected using potential-sweep measurements. Typical results of a potential-sweep experiment for both the TGP-H-090 and the H2315 I3 material are presented in Figs. 5 and 6. The experiments indicate the fundamental differences of the cell behavior in the two-phase regime. A thermostat kept the cell temperature at 313 K. Flow rates of 40 ml min^{-1} dry hydrogen and 100 ml min^{-1} ambient air were used in the case of the Freudenberg paper, whereas 50 ml min^{-1} humidified hydrogen and 100 ml min^{-1} dry air were used for the Toray. This resulted in a slightly higher membrane resistance in the case of the Freudenberg paper. A scan rate of 10 mV s^{-1} was used in each case for the dynamic variation of the cell voltage. When using a Toray paper, a pronounced hysteresis behavior at high current densities is observed (Fig. 6). The hysteresis indicates a continuous change of the liquid saturation in space and time inside the GDL material which is one of the fundamental assumptions of the two-phase and multi-phase mixture transport models based on the continuum hypothesis. In the case of the Freudenberg H2315 I3 GDL, no pronounced hysteresis behavior could be observed after detailed investigation of various operating conditions. Fig. 5 represents the typical behavior of the material in the high current density regime when there is a significant amount of liquid product water in the cell. The current response to a variation of the cell voltage is characterized by frequent breakdowns of the cell voltage attributed to flooding of the cathode side.

The two different materials are characterized by similar surface contact angle and bubble points. However, the impact of the material on the cell behavior in the two-phase regime is mainly determined by internal properties and the surface data is not sufficient to predict the behavior.

Generically, the three flow regimes for the distribution of the non-wetting phase in a porous medium are viscous fingering, stable displacement and capillary fingering [24]. The regimes can be distinguished by the ratio of the viscosities of non-wetting and wetting

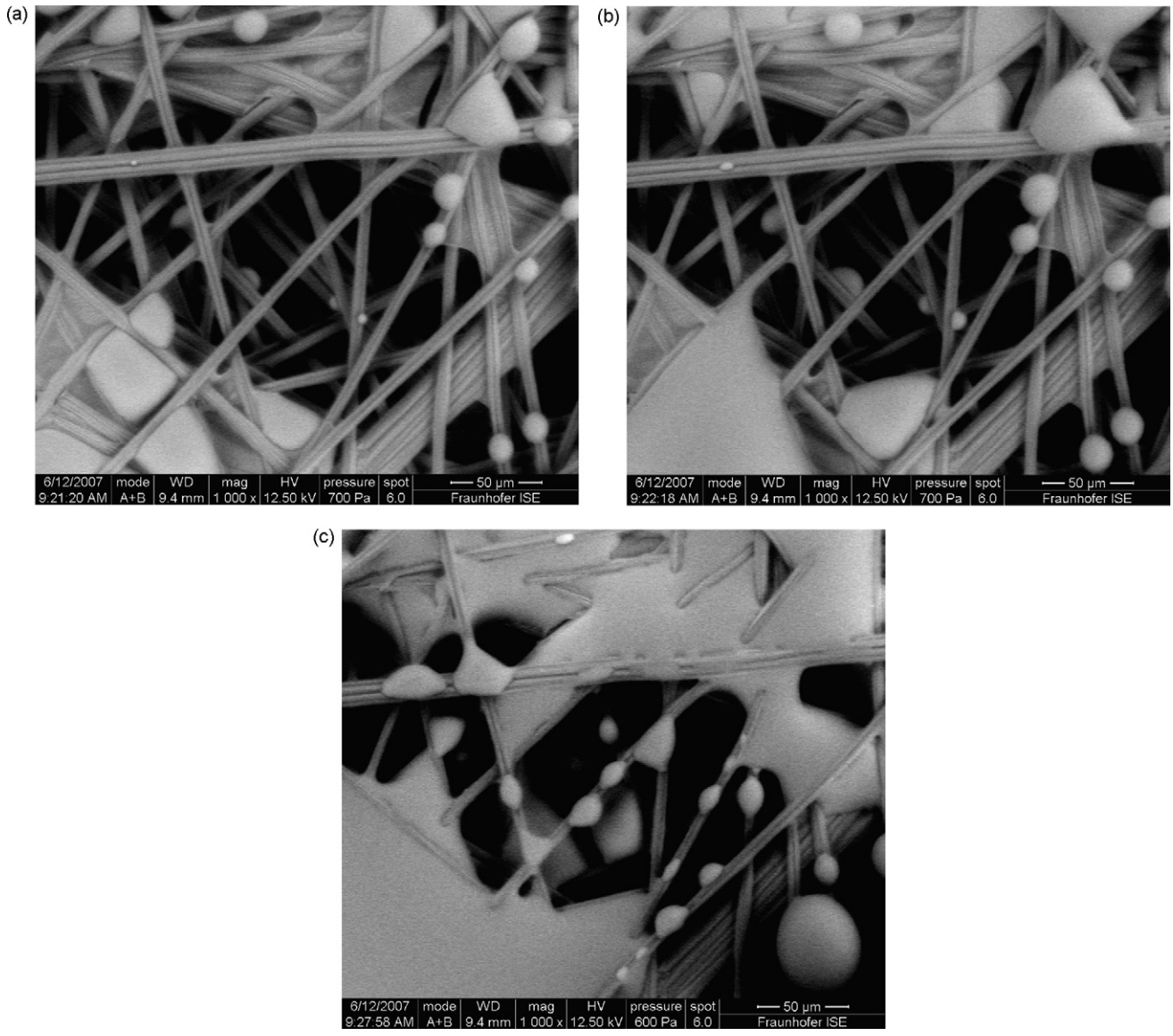

Fig. 8. In the untreated Toray TGP-H-090 GDL the droplets initially fill the hydrophilic cavities (a) and soon merge to form liquid films even at low saturation (b). Liquid films that extend over many pores are formed (c).

phases and the capillary number. The regime of stable displacement can be described to a very good approximation by the invasion of a stable front of the non-wetting phase. This is a valid model where the velocity of the non-wetting phase is comparatively large e.g. for the transport of ground-water in porous soil. The saturation profile for a purely hydrophobic medium shows fractal fingering flow. The occurrence of dead ends and the advancement of single clusters result in a concave shape of the steady-state saturation profile [25]. This is in contrast to the convex saturation profiles characteristic for stable displacement that are predicted by two-phase models (UFT and M^2) based on the continuum hypothesis. Despite PTFE treatment, hydrophilic and hydrophobic pores generally co-exist in GDL materials. Moreover, the effect of the fraction of hydrophilic pores f is studied in [25]. A Lattice Boltzmann (LB) model is used to show that the shape of the saturation profile changes from concave, which is typical for capillary fingering, to the convex form that is typical for stable front invasion when the fraction of hydrophilic pores is increased. A convex form is already observed at a hydrophilic pore fraction of 0.1. Moreover it is shown that the higher the fraction of hydrophilic pores, the higher the average liquid saturation. For $f = 0.2$, the average saturation is predicted to be approximately 0.4 assuming a current density of 2 A cm^{-2}. Two wettability scenarios are considered in [25] that show the equilibrium liquid water distribution with a purely hydrophobic GDL with a contact angle of 140° and a mixed-wettability GDL with contact angles of 80° and 140°, where a hydrophilic pore fraction of $f = 0.5$ is assumed. At a saturation level of $s_l = 0.1$ the two-phase LB model shows finely dispersed water droplets in the mixed-wettability GDL whereas fewer but larger water clusters appear in the hydrophobic GDL. The droplets merge at $s_l = 0.2$ in both cases. In case of the mixed-wettability GDL, the water distribution is film-like, forming connections between many different pores. By contrast in the hydrophobic GDL the curvature of the merged droplets is higher, resulting in a potato-like water surface that is constricted by the pore morphology.

We investigated the microscopic two-phase behavior of two different materials (Toray TGP-H-090, Freudenberg H2315 I3) using environmental scanning electron microscope (ESEM) imaging. The ESEM measurement procedure is described in detail in Ref. [26]. Under the ESEM a non-zero pressure can be maintained and hence the phase change of water in porous media is observable. The results

are shown in Figs. 7 and 8. For the Freudenberg H2315 I3 GDL, water droplets form after condensation has started at the fiber surface and start filling the cavities of the material (Fig. 7a). Subsequently, the droplets merge partially to form larger droplets (Fig. 7b), a process that continues until high saturation of the medium is reached. Eventually, a few large droplets and liquid films with high surface curvature and surface shapes governed by the pore morphology appear (Fig. 7c). In the Toray TGP-H-090 GDL the droplets formed after initial condensation fill the hydrophilic cavities (Fig. 8a) that soon merge to form liquid films even at low saturation (Fig. 8b). At high saturation, liquid films that extend over many pores are formed and a few small individual droplets formed by ongoing condensation remain. The surface curvature of the liquid phase is low and only weakly constrained by the pore morphology. This experimental evidence is in qualitative agreement with the simulation results in [25] (Fig. 12 therein). From Fig. 8 a–c it is evident that the unteflonated TGP-H-090 GDL is strongly hydrophilic, as is confirmed by Gostick et al. [23], who determined a hydrophilic pore fraction of $f = 0.81$. Hence the saturation profile for the Toray-TGP-H-090 GDL is convex. Due to the large fraction of hydrophilic pores the average saturation of the Toray GDL is likely to be higher than 0.4 as predicted in [25] for a medium having $f = 0.2$ at a liquid water injection rate corresponding to $2\,A\,cm^{-2}$. This is confirmed by the simulated saturation in Figs. 3 and 4. By contrast, the images of the Freudenberg H2315 I3 indicate that the fraction of hydrophilic pores is small. The saturation profile in such a medium is likely to be concave, contradicting existing two-phase models based on the continuum hypothesis.

A cross-link can now be established by considering the typical dynamic IV curves for both materials under investigation (Figs. 5 and 6). For materials that have a large fraction of hydrophilic pores, the saturation distribution is convex so the liquid water transport is similar to the transport regime of stable front invasion and models making use of the continuum hypothesis represent a valid approach. Accordingly, when dynamic IV curves are measured a time-continuous change of the saturation is expected when an average is taken over the GDL material [20]. Such behavior typically results in a dynamic hysteresis effect in the high current density regime. Fig. 8 c shows the evolution of a liquid film that is only weakly influenced by the pore geometry, thus enabling a transport mode that is sufficiently close to the regime of stable displacement. In case the material is dominated by a large fraction of hydrophobic pores, the transport of liquid water is expected to be dominated by capillary fingering which makes the continuum hypothesis invalid for such a case. The saturation of the GDL cannot be expected to follow a time-continuous trajectory but is likely to be governed by the evolution of single transport channels and droplets. Accordingly, the appearance of a high current density hysteresis effect is not expected. Instead, the current density is governed by a process that appears to be stochastic (Fig. 5). We relate this result to Fig. 7 c where even a significant saturation that causes mass transport limitation remains in form of droplets and individual channels similar to the results shown in [25] for a purely hydrophobic material.

To summarize, we conclude that existing two-phase models are valid for GDL-materials that have a sufficiently high fraction of hydrophilic pores (e.g. unteflonated Toray TGP-H-090, $f = 0.81$). Materials with a high fraction of hydrophobic pores cannot be described accurately by the current two-phase models. New approaches combining a thorough description of the microscale with the capability to describe the behavior of an entire fuel cell are required for this type of material. It should be noted that the use of a two-phase model with a high contact angle ($\gg 90^\circ$), as it is often found in the literature, is contradictory. A high contact angle describes a low fraction of hydrophilic pores. The average-type two-phase models appear to be invalid in this case.

5. Conclusion

A dynamic two-phase model of a proton exchange membrane fuel cell with respect to the GDL is presented. The model contains a description of the capillary transport of liquid water through the GDL that is coupled with the oxygen diffusion and the electrochemical reaction at the cathode side. A potential step voltammetry and a sine wave testing experiment are presented. Excellent agreement between experiment and simulation is achieved for both cases. The two-phase model parameters obtained through an optimization scheme are presented. The model uses the continuum hypothesis as fundamental assumption. This is the case for all UFT and M^2 two-phase models. The liquid water saturation and velocity are described by a field representation. Models based on the continuum hypothesis predict a continuous change of the saturation with respect to space and time.

Two diffusion media with similar bubble point and surface contact angle but different fraction of hydrophilic pores are compared: Unteflonated Toray TGP-H-090 paper and hydrophobic Freudenberg H2315 I3. The Freudenberg paper has a low fraction of hydrophilic pores f compared to the untreated Toray TGP-H paper. Cyclic voltammetry measurements and ESEM images show a continuous change of the saturation with respect to time and space for the unteflonated Toray paper ($f = 0.81$). The influence of the pore morphology on the liquid water distribution is weak and the typical hysteresis behavior is found. For the hydrophobic Freudenberg H2315 I3 the liquid water distribution is strongly influenced by the pore morphology. No hysteresis indicating a time continuous behavior could be observed in the cyclic voltammograms.

UFT and M^2 two-phase models are a valid approach for diffusion media with large fraction of hydrophilic pores such as unteflonated Toray-TGP-H paper. However, homogenized two-phase models (UFT and M^2) appear to be invalid for mainly hydrophobic gas diffusion media. The UFT and M^2 models predict convex saturation profiles and are unable to describe transport that is dominated by capillary fingering. Moreover the absence of a hysteresis effect without increase of the limiting current density is not explained by UFT and M^2 models. New model approaches are required that combine an accurate description of the liquid water transport in (partially) hydrophobic porous gas diffusion media and a homogenized model formulation for efficient simulation of technically relevant fuel cell operation cycles.

Acknowledgements

The authors acknowledge the valuable support of the following people at Fraunhofer ISE: J. Hermann (optimization), T. Heilmann (chronoamperometric measurements) and R. Alink (ESEM imaging). The financial support of the German Federal Ministry of Education and Research (BMBF) under grant no. 03SF0310A is gratefully acknowledged.

References

[1] Z.H. Wang, C.Y. Wang, K.S. Chen, J. Power Sources 94 (2001) 40–50.
[2] T. Berning, N. Djilali, J. Electrochem. Soc. 150 (12) (2003) A1589–A1598.
[3] U. Pasaogullari, C. Wang, J. Electrochem. Soc. 152 (2) (2005) A380–A390.
[4] Y. Wang, C. Wang, J. Electrochem. Soc. 153 (6) (2006) A1193–A1200.
[5] E. Birgersson, M. Noponen, M. Vynnycky, J. Electrochem. Soc. 152 (5) (2005) A1021–A1034.
[6] V. Schulz, D. Kehrwald, A. Wiegmann, K. Steiner, Flow, heat conductivity, and gas diffusion in partly saturated microstructures, NAFEMS Seminar Simulation of Complex Flows (CFD).
[7] J. Nam, M. Kaviani, Int. J. Heat Transfer 46 (2003) 4595–4611.
[8] G. Lin, W. He, T. Nguyen, J. Electrochem. Soc. 151 (12) (2004) A1999–A2006.
[9] B. Markicevic, N. Djilali, Phys. Fluids 18 (2006) 033101.
[10] G. He, Z. Zhao, P. Ming, A. Abuliti, C. Yin, J. Power Sources 163 (2007) 846–852.
[11] G. He, P. Ming, Z. Zhao, A. Abudula, Y. Xiao, J. Power Sources 163 (2007) 864–873.
[12] Z. Zhan, J. Xiao, M. Pan, R. Yuan, J. Power Sources 160 (2006) 1–9.

[13] G. Luo, H. Ju, C. Wang, J. Electrochem. Soc. 154 (3) (2007) B316–B321.
[14] H. Yu, G. Luo, C.Y. Wang, J. Electrochem. Soc. 154 (2) (2007) B218–B228.
[15] A. Shah, G. Kim, P. Sui, D. Harcey, J. Power Sources 163 (2007) 793–806.
[16] C. Ziegler, H. Yu, J. Schumacher, J. Electrochem. Soc. 152 (2005) A1555–A1567.
[17] H. Yu, C. Ziegler, J. Electrochem. Soc. 153 (3) (2006) A570–A575.
[18] D. Natarajan, T. Nguyen, J. Electrochem. Soc. 148 (12) (2001) A1324–A1335.
[19] H. Ju, G. Luo, C. Wang, J. Electrochem. Soc. 154 (2) (2007) B218–B228.
[20] C. Ziegler, T. Heilmann, D. Gerteisen, J. Electrochem. Soc. 155 (4) (2008) B349–B355.
[21] Y. Wang, C. Wang, J. Electrochem. Soc. 154 (7) (2007) B636–B643.
[22] J. Hermann, C. Ziegler, J. Electrochem. Soc., 155 (10) (2008) B1066–B1076.
[23] J. Gostick, M. Fowler, M. Ioannidis, M. Pritzker, Y. Volfkovitch, A. Sakars, J. Power Sources 156 (2) (2006) 375–387.
[24] R. Lenormand, E. Touboul, C. Zarcone, J. Fluid Mech. 189 (1998) 165.
[25] P. Sinha, P. Mukherjee, C. Wang, J. Mater. Chem. 17 (2007) 3053–3272.
[26] H. Yu, C. Ziegler, M. Oszcipok, M. Zobel, C. Hebling, Electrochim. Acta 51 (2006) 1199–1207.